Surface ozone and its precursors at Summit, Greenland: comparison between observations and model simulations

Yaoxian Huang[1,a], Shiliang Wu[1,2,3], Louisa J. Kramer[1,2,b], Detlev Helmig[4], and Richard E. Honrath[1,2,†]

[1]Department of Geological and Mining Engineering and Sciences, Michigan Technological University, Houghton, Michigan, USA

[2]Atmospheric Sciences Program, Michigan Technological University, Houghton, Michigan, USA

[3]College of Environmental Science and Engineering, Ocean University of China, Qingdao, China

[4]Institute of Arctic and Alpine Research, University of Colorado, Boulder, Colorado, USA

[a]now at: Department of Climate and Space Sciences and Engineering, University of Michigan, Ann Arbor, Michigan, USA

[b]now at: University of Birmingham, Birmingham, UK

[†]deceased

Correspondence to: S. Wu (slwu@mtu.edu) and Y. Huang (yaoxianh@mtu.edu)

Abstract. Recent studies have shown significant challenges for atmospheric models to simulate tropospheric ozone (O_3) and some of its precursors in the Arctic. In this study, ground based data are combined with a global 3-D chemical transport model (GEOS-Chem) to examine the abundance and seasonal variations of O_3 and its precursors at Summit, Greenland (72.34˚ N, 38.29˚ W, 3212 m.a.s.l). Model simulations for atmospheric nitrogen oxides (NO_x), peroxyacetyl nitrate (PAN), ethane (C_2H_6), propane (C_3H_8), carbon monoxide (CO), and O_3 for the period of 07/2008-06/2010 are compared with observations. The model performs well in simulating certain species (such as CO and C_3H_8), but some significant discrepancies are identified for other species and further investigated. The model generally underestimates NO_x and PAN (by ~ 50% and 30%, respectively) for March-June. Likely contributing factors to the low bias include missing NO_x and PAN emissions from snowpack chemistry in the model. At the same time, the model overestimates NO_x mixing ratios by more than a factor of two in wintertime, with episodic NO_x mixing ratios up to 15 times higher than the typical NO_x levels at Summit. Further investigation shows that these simulated episodic NO_x spikes are always associated with

transport events from Europe, but the exact cause remains unclear. The model systematically overestimates C_2H_6 mixing ratios by approximately 20% relative to observations. This discrepancy can be resolved by decreasing anthropogenic C_2H_6 emissions over Asia and the US by ~ 20%, from 5.4 to 4.4 Tg/yr. GEOS-Chem is able to reproduce the seasonal variability of O_3 and its spring maximum. However, compared with observations, it underestimates surface O_3 by approximately 13% (6.5 ppbv) from April to July. This low bias appears to be driven by several factors including missing snowpack emissions of NO_x and nitrous acid in the model, the weak simulated stratosphere-to-troposphere exchange flux of O_3 over the summit, as well as the coarse model resolution.

1. Introduction

Tropospheric ozone (O_3) and its precursors, including nitrogen oxides (NO_x = NO + NO_2), carbon monoxide (CO), and volatile organic compounds (VOCs, such as ethane, propane, etc.) are important atmospheric species affecting both air quality and climate (e.g., Jacob et al., 1992; Fiore et al., 2002; Unger et al., 2006; Hollaway et al., 2012). Tropospheric O_3 is mainly produced by photochemical oxidation of CO and VOCs in the presence of NO_x, with additional contribution by transport from the stratosphere. Its major sinks include chemical reactions and dry deposition. As a reservior species for NO_x, peroxyacetyl nitrate (PAN) also plays an important role in atmospehric chemistry. PAN and O_3, as well as some of their precursors, have relatively long lifetimes in the atmosphere, enabling them to be transported long distance to remote regions such as the Arctic.

Recent studies have shown some significant challenges for atmospheric chemical transport models to simulate O_3 and its precursors in the Arctic (e.g., Shindell et al., 2008; Alvarado et al., 2010; Walker et al., 2012; Wespes et al., 2012; Fischer et al., 2014; Monks et al., 2015), but the causes remain unclear. In the multi-model assessment by Shindell et al. (2008), more than a dozen models all showed systematic and persistent underestimation of O_3 at the GEOSummit station, Greenland (hereafter referred to as Summit). Alvarado et al. (2010) used NO_x and PAN measurements from the ARCTAS (Arctic Research of the Composition of the Troposphere from Aircraft and Satellites) mission in the summer to compare with model simulations. They found that model simulated NO_x mixing ratios were higher than observations, while PAN mixing ratios were lower than the observations in fresh boreal fire plumes. In terms of global PAN

simulations, Fischer et al. (2014) directly partitioned 40% of NO_x emissions from wildfires to PAN formation, which improved the agreement between model and observations. However, the model still underestimated PAN surface mixing ratios during springtime in the Arctic. Walker et al. (2012) reported that model simulated O_3 mixing ratios were biased low when compared with balloon data during summertime from two high-latitude sites at Eureka (80˚N, 86˚W) and Ny-Ålesund (79˚, 12˚E). Wespes et al. (2012) also revealed that model simulated O_3 mixing ratios within the boundary layer were significantly underestimated during spring-summer, compared with ARCTAS measurements. More recently, Monks et al. (2015) further demonstrated that model simulated O_3 mixing ratios in the Arctic at the surface and in the upper troposphere were generally lower than the observations. In addition, a recent study by Christian et al. (2017) compared O_3 observations from the ARCTAS campaign to GEOS-Chem model simulations and found consistent low biases with the model simulated O_3 at all altitudes except the surface.

Field measurements at Summit show that the snowpack emits gas-phase NO_x, PAN, nitrous acid (HONO), as well as hydrogen peroxide (H_2O_2) during spring-summer, when polar sun rises (Ford et al., 2002; Honrath et al., 2002). Although several 1-D models (Thomas et al., 2011, 2012; Frey et al., 2013; Murray et al., 2015) have validated the importance of snowpack emissions for surface NO_x as well as O_3 formation, current global chemical transport models (CTMs) usually do not include these emission sources (Zatko et al., 2016).

In this study, we examine the abundance and seasonal variations of O_3 and its precursors at Summit with a global chemical transport model, GEOS-Chem CTM, in conjunction with two years of in-situ measurement data for 2008-2010. We first evaluate the model performance in simulating surface O_3 and its precursors, and then implement a series of model updates to resolve the identified model biases. This paper is organized as follows: section 2 describes model methods and observations, followed by detailed comparisons of model simulations against observations for O_3 and O_3 precursors in section 3; conclusions are summarized in section 4.

2. Observational data and model simulations

In situ measurements of NO_x, PAN, and non-methane hydrocarbons (NMHCs) were performed at Summit from July 2008 to June 2010 (Helmig et al., 2014b; Kramer et al., 2015). An automated chemiluminescence instrument was used to measure NO_x (Ridley and Grahek, 1990);

a commercial PAN gas chromatography analyzer (PAN-GC, Metcon, In., Boulder, CO) was employed for the measurement of PAN. Measurements of NMHC relied on an automated Gas Chromatography-Flame Ionization Detection (GC-FID) system. Readers are referred to Kramer et al. (2015) and Helmig et al. (2014b) for the details of the measurement techniques and equipment setup. Surface measurements of O_3 using ultraviolet light absorption (Petropavlovskikh and Oltmans, 2012), and CO by GC (Novellie and Masarie, 2015) are from the National Oceanic and Atmospheric Administration (NOAA). Hourly averaged O_3, and flask data for CO between July 2008 and June 2010 were downloaded from the NOAA Earth System Research Laboratory (ESRL) Global Monitoring Division (GMD) website (http://www.esrl.noaa.gov/gmd/dv/data/). Vertical ozonesonde data profiles were also downloaded from NOAA ESRL GMD (McClure-Begley et al., 2014).

Simulations of O_3 and related species (NO_x, PAN, NMHCs) are conducted using the GEOS-Chem model (Bey et al., 2001) with coupled O_3-NO_x-VOC-Aerosol chemistry mechanism (i.e. these species interact with each other in the model). The GEOS-Chem CTM is driven by assimilated meteorological data from the Goddard Earth Observing System version 5.2.0 (GEOS-5.2.0) of the NASA Global Modeling Assimilation Office. The GEOS-Chem model has been extensively evaluated and applied in a wide range of applications (Martin et al., 2002; Park et al., 2004; Wu et al., 2007; Hudman et al., 2009; Johnson et al., 2010; Huang et al., 2013; Kumar et al., 2013; Zhang et al., 2014; Hickman et al., 2017), including the studies in the Arctic (e.g., Alvarado et al., 2010; Monks et al., 2015; Christian et al., 2017). GEOS-Chem v10-1 with grid resolution of 4˚ latitude by 5˚ longitude, and 47 vertical layers was used for the model control simulation. Following McLinden et al. (2000), the Linoz stratospheric O_3 chemistry scheme was used. The simulation was run from June 2007 to June 2010 and the results from the last two years were used in the final analysis. Time series data were archived with 3-hr temporal resolution at the Summit grid box.

Global anthropogenic emissions of NO_x, SO_2, NH_3, and CO in the model are based on the Emission Database for Global Atmospheric Research (EDGAR) v4.2 inventory, which is overwritten by regional emission inventories where applicable, such as the BRAVO inventory for Mexico (Kuhns et al., 2005), the CAC over Canada, the EMEP emissions over Europe, the Model Inter-comparison Study for Asia Phase III (MIX) emissions over Asia (Li et al., 2017),

and the US EPA NEI 2011 (NEI11) emission inventory (Simon et al., 2010). The soil NO_x emission scheme follows Hudman et al. (2012). Lightning NO_x emissions are calculated per flash rate based on GEOS-5 computed cloud-top heights (Price and Rind, 1992), which are determined by deep convection and constrained by satellite observations for monthly average flash rates from the Lightning Imaging Sensor and Optical Transient Detector (OTD/LIS) (Sauvage et al., 2007; Murray et al., 2012). Biomass burning emissions are from the Global Fire Emission Database version 4 (GFED4) inventory with monthly resolution (Giglio et al., 2013). The RETRO (Reanalysis of the TROpospheric chemical composition) global anthropogenic NMHC emission inventory (van het Bolscher et al., 2008) was used except for ethane (C_2H_6) and propane (C_3H_8), which follows Xiao et al. (2008, hereafter referred to as X08) for the year 2001. Global biofuel emission inventory follows Yevich and Logan (2003), which includes emissions for C_2H_6 and C_3H_8. For biogenic VOC emissions, the Model of Emissions of Gases and Aerosols from Nature (MEGAN) scheme (Guenther et al., 2006) was used. Dry deposition of species in GEOS-Chem uses a standard resistance-in-series scheme (Wesely, 1989), as implemented in Wang et al. (1998). Wet scavenging follows Liu et al. (2001), including scavenging in convective updraft, rainout (in-cloud) and washout (below-cloud) from convective anvils and large-scale precipitation.

We first run the standard GEOS-Chem model with a-priori emissions and compare the simulation results against observations for various species (including NO_x, PAN, C_2H_6, C_3H_8, CO, and O_3, as shown in Fig. 1). Then we focus on the model-observation discrepancies, and where applicable, make revisions to the model simulations and further evaluate the improvement in model performance, as discussed in details below.

3. Results and Discussions

3.1 NO_x

We first combine the two years of data for July 2008 – June 2010 and anylaze their seasonal variations. As shown in Figure 1a, the GEOS-Chem model simulated NO_x agree well with the observations for July-October. However, compared to observations, the model results significantly overestimate NO_x mixing ratios for November-January by about 150%, while underestimating the data in spring and early summer by approximately 60%. Another challenge

for the model simulation is that it does not capture the decrease of NO_x for May - November. We find that during the 2009-2010 winter season, model simulations show several high NO_x spikes with peak NO_x mixing ratios reaching ~ 0.15 ppbv or higher, which is ~ 15 times greater than typical backgound levels (Fig. 2). These large peaks in NO_x were not observed in the data. Similar peaks were also seen in the model simulations during the 2008-2009 winter season; however, there are no measurements available for this period to compare with.

Further analyses show that the model-simulated high NO_x spikes during wintertime are all associated with transport events from Europe. We carry out a sensitivity study to examine the impacts of European emissions on Arctic NO_x by manually reducing anthropogenic NO_x emissions from the EMEP emission inventory over Europe by 50% (EMEP50). Results show that surface peak NO_x mixing ratios over Summit during the spike events (e.g., dates around 12/09/2009, 12/15/2009, 1/15/2010 and 1/22/2010) from EMEP50 almost decline proportionally by ~ 50% during 2009/12/01-2010/01/31 (Fig. 2), which confirms that the modeled NO_x spikes at Summit during wintertime are associated with transport from Europe. However, the model simulated NO_x is still significantly higher than observations. Comparisons for surface NO_2 mixing ratios between model simulations and 11 in-situ observational sites over Europe during this period were conducted with data downloaded from http://ebas.nilu.no. For detailed site information, NO_2 measurement technique and resolution, refer to Table 1. Measurment data over these two months for each site were averaged to compare with the corresponding grid cell in the model. As shown in Figure 3a, GEOS-Chem overestimates surface NO_2 mixing ratios at these sites by over 66%, compared with observations (slope=1.07; correlation coefficient=0.88).

Instead of using EMEP, we carry out another sensitivity study to force anthropogenic NO_x emissions over Europe following EDGAR v4.2 (EURO_EDGAR), with other model configurations identical to control simulations. As shown in Figure 2, the NO_x mixing ratios over Summit during 12/2009-01/2010 agree much better with observations, especially for January 2010, where the model captures the magnitudes of observational peaks. This is because NO_x emissions from EDGAR over Europe (1.97 Tg NO) are 12% lower than those from EMEP (2.24 Tg NO) for the months of 12/2009 and 01/2010. Furthermore, the discrepancy for the differences of surface NO_2 mixing ratios over Europe between EURO_EDGAR and observations is further reduced (by 50%), relative to the control runs, with a model-to-observation slope of 0.92 and a

correlation coefficient of 0.83 (Fig. 3b). Similarly, we also tested the sensitivty of surface NO_x mixing ratios over Summit in response to the changes in the anthropogenic NO_x emissions from NEI11 over US and MIX over Asia (including Siberia) during these two months, and found that surface NO_x mixing ratios over Summit during these two months were quite close to the control simulations (not shown), reflecting insenstivity to emission perturbations from the US and Asia. Therefore, we conclude that uncertainties in fossil fuel NO_x emissions of EMEP associated with transport events from Europe in the model are the most likely cause for the wintertime NO_x spikes over Summit.

For April-July, model simulated monthly mean NO_x mixing ratios over Summit are a factor of two lower than the observations (Fig. 4a). In-situ measurements at Summit by Honrath et al. (1999, 2000a, 2000b, 2002) showed upward fluxes of NO_x (2.52×10^8 molecules cm^{-2} s^{-1}) from photolysis of nitrate in snowpack during the summertime, leading to enhancement in NO_x levels in the surface layer by approximately 20 pptv, which is comparable to surface NO_x mixing ratios in the Arctic from other sources. Similar results were found over the East Antarctic Plateau snow/ice sheet (Frey et al., 2013; Legrand et al., 2014). The standard GEOS-Chem model does not include the photolysis of nitrate from snowpack, implying a missing source for NO_x in the Arctic/Antarctic boundary layer.

In order to test the sensitivity of model simulated surface NO_x mixing ratios to the snowpack emissions, we implement in the model a constant NO_x flux of ~ 2.52 x 10^8 molecules cm^{-2} s^{-1} during April-July over Greenland (60-85° N, 20-60° W), following the measurements conducted at Summit during summertime by Honrath et al. (2002). As a result, we find that on average, the model simulated surface NO_x mixing ratios for April to July over Summit more than double that from the control simulation, which improves the agreement between model and observations for April-June (Fig. 4a). However, the assumed NO_x flux from snowpack in the model leads to overestimate of NO_x mixing ratios in July and the model is still not able to reproduce the decreasing trend of NO_x for May-October. This decreasing trend of NO_x may be driven by the decreasing NO_x production rate in snowpack resulting from a gradual depletion of snowpack NO_x reservoir (Van Dam et al., 2015), which is not reflected in the model since we implement a simple constant NO_x emission flux. Dibb et al. (2007) reported that nitrate concentrations in the Summit snowpack peaked in June and declined toward fall by ~ 1/3. Van Dam et al. (2015)

further showed decreasing trend for NO_x mixing ratios within the snowpack at Summit from June to October. This may partially explain why we would see the declining trend of surface NO_x mixing ratios over Summit from June toward fall. The NO_x emissions from snowpack are affected by a number of factors including nitrate concentrations and solar radiation available and the responses can be very non-linear. Further investigations are needed to account for the seasonal variations of snowpack NO_x emissions from nitrate photolysis in the model, i.e., constrained by seasonal snowpack NO_x emission flux measurements in the future.

3.2 PAN

We then examine the model performance for PAN, which serves as a reservoir for NO_x. Figure 1b shows the comparison of model simulated monthly mean PAN mixing ratios with the measurement data. The model captures the seasonal variation of PAN well, although significantly (by ~ 30%) underestimting the PAN mixing ratios for April-June. By running the model simulation with higher horizontal resolution at 2° latitude by 2.5° longitude (hereafter referred to as GEOS-Chem 2x2.5), we find that the monthly mean PAN mixing ratios over Summit during April-July increased by up to 23.3 pptv compared to the 4x5 simulation (Fig. 4b). This can be explained by two reasons. First, coarse model resolution (e.g., 4x5 horizontal resolution) could artificially smear the intense emission sources throughout the entire grid cell (e.g., over urban regions), leading to underestimates of downwind concentrations for species, e.g., O_3 and O_3 precursors (Jang et al., 1995; Yu et al., 2016). Second, ventilation of the lower atmosphere could be better resolved by a finer model resolution, leading to more efficient vertical advection (Wang et al., 2004; Chen et al., 2009; Yu et al., 2016). However, on average, monthly mean model simulated PAN mixing ratios are still underestimated by 20% during this period, compared with observations. This is consistent with the study by Arnold et al. (2015), which reported that model simulated PAN mixing ratios in GEOS-Chem were lower than ARCTAS observations over high-latitude atmosphere in the Arctic. Meanwhile, this study also revealed that GEOS-Chem produced less PAN relative to CO in Arctic air parcels that were influenced by fires, compared with other models.

Snowpack can emit not only NO_x, but also PAN, based on field studies at Summit during summertime by Ford et al. (2002). GEOS-Chem does not contain snowpack PAN emissions and

chemistry. For a sensitivity study, similar to snowpack NO_x emissions as discussed in section 3.1, we consider a 24-hr constant flux of 2.52 x 10^8 molecules cm^{-2} s^{-1} of PAN over Greenland from April to July, following Ford et al. (2002). As a result, model simulated PAN mixing ratios agree much better with observations (Fig. 4b). Note that there are also other possible reasons that lead to model bias. For instance, a study by Fischer et al. (2014) showed improved agreement between modeled and measured PAN in the high latitudes when assignining a portion of the fire emissions in the model above the boundary layer and also directly partitioning 40% of NO_x emissions from fires into PAN. We carried out a sensitivity test with similar treatments, but no significant improvements in the model simulated surface PAN were observed at the Summit site. Therefore, we did not include the PAN updates from Fischer et al. (2014) in other model simulations in this study.

3.3 NMHC

Comparisons of observed surface C_2H_6 and C_3H_8 mixing ratios with GEOS-Chem simulations at Summit are shown in Figures 1c and 1d. The model simulations agree well with surface measurements of C_3H_8, but systematically overestimate C_2H_6 (by approximately 25% annually), with the largest bias (0.48 ppbv) occuring during summer. This is consistent with the study from Tzompa-Sosa et al., (2017), which used the same model as our study and pointed out that using X08 as global anthropogenic C_2H_6 emission inventory systematically overestimated surface C_2H_6 mixing ratios over the Northern Hemisphere, compared with ground-based observations. Anthropogenic C_2H_6 emissions over US from NEI11 are shown to geographically match the distribution of active oil and natural wells (Tzompa-Sosa et al., 2017), and the most recent MIX has been updated to synergize anthropogenic C_2H_6 emissions from various countries over Asia (Li et al., 2017). Therefore, instead of using global anthropogenic fossil fuel emissions of C_2H_6 following X08, we first conduct sensitivity simulations by overwritting global emission inventories by NEI11 over the US, and MIX over Asia (hereafter referred to as NEI11_MIX). Both NEI11 and MIX contain emissions for the years from 2008 to 2010, which could realistically represent the annual and seasonal variations of C_2H_6 emissions over the US and Asia, thus spatially and temporally better representative of anthropogenic C_2H_6 emissions from mid-latitudes transported to the Arctic regions. In general, model control simulations overestimate annual mean surface C_2H_6 mixing ratios primarily in the Northern Hemisphere,

with large differences occurring over Asia and the US by up to 5 ppbv, compared with NEI11_MIX during the period of 07/2008-06/2010 (Fig. S1). All the above changes are driven by the substantial reductions of anthropogenic C_2H_6 emissions between emission inventories, from 3.5 (X08) to 2.5 Tg/yr (MIX) over Asia, and from 1.9 Tg/yr (X08) to 1.4 Tg/yr (NEI11) over US, reflecting the decreasing trend of anthropogenic C_2H_6 emissions during 2001-2009 (Helmig et al., 2014a), because the X08 emission inventory is based on the year 2001. Substantial changes in surface C_2H_6 mixing ratios over the US bewteen control simulations and NEI11_MIX reflect that there exist tempospatial changes of C_2H_6 emissions from oil and gas productions during the period of 2001-2009. A similar pattern was also found by Tsompa-Sosa et al. (2017). In contrast to the control simulations, NEI11_MIX model simulations show that monthly mean C_2H_6 mixing ratios over Summit are systematically underestimated by 24%, compared with observations (Fig. 5). Tsompa-Sosa et al. (2017) reported that NEI11 for C_2H_6 emissions were likely underestimated by 40%, compared with in-situ and aircraft observations over the US. We therefore run a sensitivity simulation by increasing the NEI11 C_2H_6 emissions by 40% and keeping other model configuration identical to NEI11_MIX (hereafter referred to as NEI11_40_MIX). We find this update leads to an increase in the model simulated annual mean surface C_2H_6 mixing ratios over Summit by only 6% during the period of 07/2008-06/2010 (figure not shown), still not able to explain the high model bias.

Similar to NEI11_MIX, we further conduct sensitivity studies by only replacing the regional emission inventory for C_2H_6 over the US, with other regions still following X08 (hereafter referred to as NEI11_ONLY). Consequently, model simulated surface C_2H_6 mixing ratios over Summit agree better with observations during winter-spring (Fig. 5), decreasing the bias from +15% (control simulations) to +6%. However, model simulated C_2H_6 mixing ratios during summer-fall are higher than the observations by over 30%.

We then scale up the MIX emissions for C_2H_6 by 20% over Asia, with other model configurations identical to NEI11_MIX (hereafter referred to as NEI11_MIX20). By doing this, we increase fossil fuel C_2H_6 emissions from 2.5 to 3 Tg/yr. We find that the simulated annual mean surface C_2H_6 mixing ratios at Summit from NEI11_MIX20 agree quite well with observations (within 1%). Similarly, better agreement between model and observations are found for monthly average values for October - January. However, the new simulation is not able to

reproduce the seasonal cycle of C_2H_6 - the model signficantly underestimates in February – April but overestimates in June – September (Fig. 5). This implies that further assessments of anthropogenic C_2H_6 emissions from MIX over Asia are needed and a more accurate global anthropogenic C_2H_6 emission inventory should be developed and validated to replace X08 in the future. Note that this standard version of GEOS-Chem does not account for the sink of C_2H_6 from the reaction with chlorine, which could reduce the global annual mean surface C_2H_6 mixing ratios by 0-30%, and the global burden of C_2H_6 by about 20% (Sherwen et al., 2016). This may introduce additional uncertainty for our measurement-model comparison, together with uncertainty in the seasonality of C_2H_6 chemistry.

3.4 CO

Figure 1e shows the comparison of model simulated CO mixing ratios with observations over Summit. Overall, the model generally captures the abundance and seasonal variation of CO. Compared with observations, the annual mean CO mixing ratio is slightly overestimated by about 3 ppbv in the model.

3.5 O_3

Surface O_3 mixing ratios from model simulations and surface observations are compared in Figure 1f. The GEOS-Chem model captures the seasonal variation of O_3 including the spring peak. However, the model shows a systematic low bias for most of the year, in particualr for April–July when the surface O_3 mixing ratios are underestimated by ~ 13% (~ 6.5 ppbv). Here we focus our analysis for the possible causes that lead to the model low bias during April-July.

As discussed earlier, snowpack emissions due to the photolysis of nitrate in the snow during late spring and summer could contribute to NO_x and HONO levels in the ambient air, which could enhance O_3 production (Crawford et al., 2001; Zhou et al., 2001; Dibb et al., 2002; Honrath et al., 2002; Yang et al., 2002; Grannas et al., 2007; Helmig et al., 2008; Legrand et al., 2014). We run a sensitivity study to test the response of surface O_3 mixing ratios to the perturbations of NO_x and HONO from snowpack emissions. In addtion to snowpack NO_x emissions that are described in Section 3.1, we implement in the model a constant flux of HONO (4.64×10^7 molecules cm^{-2} s^{-1}) from April to July (Honrath et al., 2002). As a result, monthly mean model simulated surface O_3 mixing ratios increased by up to 3 ppbv during this period (Fig. 6). The largest effect occurs

in July due to relatively strong solar radiation. O_3 formation due to snowpack emissions in our study is slightly higher than that in Zatko et al. (2016) because HONO from snowpack emissions is not considered in their study. However, for the months of April and May, surface O_3 mixing ratios only increase by ~ 1 ppbv, compared with the control runs. That is, even after accounting for the snowpack emissions, the model simulated O_3 mixing ratios are still significantly lower than the observations.

Comparison of the model simulations at different resolutions (4x5 vs. 2x2.5) shows that the finer resolution simulations substantially increase monthly mean O_3 mixing ratios over Summit by up to 6 ppbv for the months of June and July (Fig. 6). As discussed in section 3.2, fine model resolution can better resolve the emission strengths, which could significantly affect downwind chemical reactions, e.g., O_3 production efficiency (Liang and Jacobson, 2000). Moreover, terrain elevations from fine model resolution are better represented (thus better representative of Summit's elevation) and more efficient vertical ventilation of O_3 and O_3 precursors can be achieved (Wang et al., 2004). Together with the impact of snowpack chemistry, this brings model simulated surface O_3 mixing ratios over Summit to much better agreement with observations for June - July. However, there is still a low bias in the model for the months of April and May.

Another possible cause for the low O_3 biases in model simulations is the calculated stratosphere-to-troposphere exchange (STE) O_3 flux in the model. Liang et al. (2011) have pointed out that STE could be a significant direct sources of O_3 in the Arctic during spring - summer. We retrieve vertical profiles of O_3 mixing ratios and specific humidity from ozonesondes (0-5 km elevation above the Summit surface) launched at Summit for the months of June and July in 2008 and compare those data with model control runs. Ozonesondes were launched intensively during these two months (a total of 19 times). As shown in Figure 7, compared with observations, model simulated O_3 mixing ratios averaged over 0-5 km above ground level are underestimated by 3% and 9% in June and July 2008 (Fig. 7a). However, specific humidity in GEOS-5 is overestimated by 50% and 81% (Fig. 7b) respectively. Ozonesonde data show that Summit frequently encounters high O_3/low water vapors events (e.g., July 9-11, 2008), which are likely of upper tropospheric/stratospheric origin (Helmig et al., 2007b), but these are not captured by the model, which implies that GEOS-Chem possibly underestimates STE for O_3 over Summit.

This is consistent with the study by Choi et al. (2017), which found low bias with model simulated O_3 mixing ratios over high-latitude upper troposphere of the Northern Hemisphere, compared with ozonesonde data, and attributed the low bias to weak STE in the model.

Boundary layer height is another factor that could lead to model-data discrepancy in O_3 mixing ratios (Grannas et al., 2007; Helmig et al., 2007a, c). The mean springtime afternoon (12:00-14:00, local time) boundary layer height in the model at Summit for the year 2009 is 160 m, which agrees fairly well with observations (156 m) at Summit conducted in spring 2005 (Cohen et al., 2007). Therefore, we exclude that model uncertainties in boundary layer height representation in springtime cause the low bias of O_3 mixing ratios between model and observations.

4. Conclusions

We combine model simulations with two-year (July 2008 - June 2010) ground based measurements at Summit, Greenland, to investigate the abundance and seasonal variations of surface O_3 and related species in the Arctic. In general, the GEOS-Chem model was capable of reproducing the seasonal cycles of NO_x, PAN, C_2H_6, C_3H_8, CO, and O_3. However, some major discrepancies between model and observations, especially for NO_x, PAN, C_2H_6, and O_3 were identified.

There are significant differences between model simulated NO_x mixing ratios and observations for the spring and winter seasons. The model underestimates NO_x mixing ratios by approximately 50% during late spring to early summer, which is likely due to the missing NO_x emissions from nitrate photolysis in the snowpack. At the same time, the model overestimates NO_x mixing ratios by more than a factor of two in wintertime. Model simulations indicate episodic but frequent transport events from Europe in wintertime leading to NO_x spikes reaching 15 times typical NO_x mixing ratios at Summit; these large NO_x spikes are not seen in the observations. We have carried out multiple sensitivity model studies but are still unable to fully reconcile this discrepancy.

The model successfully captures the seasonal cycles and the spring maximum PAN mixing ratios, although it underestimates PAN by over 30% during late spring and early summer. Model

sensitivity studies reveal that this discrepancy could be largely resolved by accounting for PAN emissions from snowpack.

For C_3H_8 and CO, model simulations overall agree well with the surface measurements. However, the model tends to systematically overestimate surface C_2H_6 mixing ratios by ~20% on an annual average, compared with observations. This may be explained by that annual emission budgets of C_2H_6 over US and Asia from X08 emission inventory are higher than those from NEI11 and MIX by over 40%. By replacing X08 over the US with NEI11 for C_2H_6, and scaling up MIX by 20%, the model-observation bias can be resolved, resulting in an annual mean bias of less than 1%. However, care must be taken to interpret this result because we do not take into account other factors that may influence the discrepancy of surface C_2H_6 mixing ratios at Summit between model and observations, such as the C_2H_6 chemistry with chlorine.

GEOS-Chem is able to reproduce the seasonal variation of surface O_3 at Summit but persistently underestimates O_3 mixing ratios by ~ 13% (~ 6.5 ppbv) from April to July. This low bias is likely caused by a combination of misrepresentations, including the missing snowpack emissions of NO_x and HONO, inaccurate representation of Summit's elevation with a too coarse model resolution, as well as the underestimated STE.

All the results presented above reveal the importance of local snowpack emissions in regulating the air quality over the Arctic. Improvements in global CTM could likely be achieved by coupling snowpack emissions of reactive gases and photochemistry modules in order to better simulate O_3 and O_3 precursors over snow and ice (Zatko et al., 2016). Moreover, this study also demonstrates that anthropogenic emissions from midlatitudes play an important role in affecting the Arctic air quality.

Acknowledgements This research was funded by U.S. EPA grant 83518901. Findings are solely the responsibility of the grantee and do not necessarily represent the official views of the U.S. EPA. Further, U.S. EPA does not endorse the purchase of any commercial products or services mentioned in the publication. Superior, a high performance computing cluster at Michigan Technological University, was used in obtaining results presented in this publication. L. J. Kramer, D. Helmig and R. E. Honrath thank NASA (grant NNX07AR26G) for supporting the measurements at Summit. S. Wu acknowledges the sabbatical fellowship from the Ocean

University of China. We acknowledge the observational dataset of O_3 and CO provided by NOAA ESRL. Technical supports from M. Sulprizio and C. Keller are also acknowledged.

References

Alvarado, M. J., Logan, J. A., Mao, J., Apel, E., Riemer, D., Blake, D., Cohen, R. C., Min, K.-E., Perring, A. E., Browne, E. C., Wooldridge, P. J., Diskin, G. S., Sachse, G. W., Fuelberg, H., Sessions, W. R., Harrigan, D. L., Huey, G., Liao, J., Case-Hanks, A., Jimmenez, J. L., Cubison, M. J., Vay, S. A., Weinheimer, A. J., Knapp, D. J., Montzka, D. D., Flocke, F. M., Pollack, I. B., Wennberg, P. O., Kurten, A., Crounse, J., St. Clair, J. M., Wisthaler, A., Mikoviny, T., Yantosca, R. M., Carouge, C. C., and Le Sager, P.: Nitrogen oxides and PAN in plumes from boreal fires during ARCTAS-B and their impact on ozone: an integrated analysis of aircraft and satellite observations, Atmos. Chem. Phys., 10, 9739-9760, doi:10.5194/acp-10-9739-2010, 2010.

Arnold, S. R., Emmons, L. K., Monks, S. A., Law, K. S., Ridley, D. A., Turquety, S., Tilmes, S., Thomas, J. L., Bouarar, I., Flemming, J., Huijnen, V., Mao, J., Duncan, B. N., Steenrod, S., Yoshida, Y., Langner, J., and Long, Y.: Biomass burning influence on high-latitude tropospheric ozone and reactive nitrogen in summer 2008: a multimodel analysis based on POLMIP simulations, Atmos. Chem. Phys., 15, 6047-6068, doi:10.5194/acp-15-6047-2015, 2015.

Bey, I., Jacob, D. J., Yantosca, R. M., Logan, J. A., Field, B. D., Fiore, A. M., Li, Q., Liu, H., Mickley L. J., and Schultz, M. G.: Global modeling of tropospheric chemistry with assimilated meteorology: Model description and evaluation, J. Geophys. Res.-Atmos., 106, 23073-23095,

437 2001.
438 Chen, D., Wang, Y., McElroy, M. B., He, K., Yantosca, R. M., and Le Sager, P.: Regional CO
439 pollution and export in China simulated by the high-resolution nested-grid GEOS-Chem
440 model, Atmos. Chem. Phys., 9, 3825–3839, doi:10.5194/acp-9-3825-2009, 2009.
441 Choi, H., Liu, H., Crawford, J. H., Considine, D. B., Allen, D. J., Duncan, B. N., Horowitz, L.
442 W., Rodriguez, J. M., Strahan, S. E., Zhang, L., Liu, X., Damon, M. R., and Steenrod, S. D.:
443 Global O_3-CO correlations in a chemistry and transport model during July-August: evaluation
444 with TES satellite observations and sensitivity to input meteorological data and emissions,
445 Atmos. Chem. Phys., 17, 8429–8452, doi:10.5194/acp-17-8429-2017, 2017.
446 Christian, K. E., Brune, W. H., and Mao, J.: Global sensitivity analysis of the GEOS-Chem
447 chemical transport model: ozone and hydrogen oxides during ARCTAS (2008), Atmos. Chem.
448 Phys., 17, 3769-3784, doi:10.5194/acp-17-3769-2017, 2017.
449 Cohen, L., Helmig, D., Neff, W., Grachev, A., and Fairall, C.: Boundary-layer dynamics and its
450 influence on atmospheric chemistry at Summit, Greenland, Atmos. Environ., 41, 5044–5060,
451 2007.
452 Crawford, J. H., Davis, D. D., Chen, G., Buhr, M., Oltmans, S., Weller, R., Mauldin, L., Eisele,
453 F., Shetter, R., Lefer, B., Ari- moto, R., and Hogan, A.: Evidence for photochemical produc-
454 tion of ozone at the South Pole surface, Geophys. Res. Lett., 28, 3641–3644, 2001.
455 Dibb, J. E., Arsenault, M., Peterson, M. C., and Honrath, R. E.: Fast nitrogen oxide
456 photochemistry in Summit, Greenland snow, Atmospheric Environment, 36, 2501-2511, 2002.
457 Dibb, J. E., Whitlow, S. I., Arsenault, M.: Seasonal variations in the soluble ion content of snow

458 at Summit. Greenland: Constraints from three years of daily surface snow samples, Atmos.
459 Environ., 41, 5007-5019, doi:10.1016/j.atmosenv.2006.12.010, 2007.
460 Fiore, A. M., Jacob, D. J., Field, B. D., Streets, D. G., Fernandes, S. D., and Jang, C.: Linking
461 ozone pollution and climate change: The case for controlling methane, Geophys. Res. Lett.,
462 29, 1919, doi:10.1029/2002GL015601, 2002.
463 Fischer, E. V., Jacob, D. J., Yantosca, R. M., Sulprizio, M. P., Millet, D. B., Mao, J., Paulot, F.,
464 Singh, H. B., Roiger, A., Ries, L., Talbot, R. W., Dzepina, K., and Pandey Deolal, S.:
465 Atmospheric peroxyacetyl nitrate (PAN): a global budget and source attribution, Atmos.
466 Chem. Phys., 14, 2679-2698, doi:10.5194/acp-14-2679-2014, 2014.
467 Ford, K. M., Shepson, P. B., Bertman, S. B., Honrath, R. E., Peterson, M., Dibb, J. E., and
468 Bottenheim, J. W.: Studies of peroxyacetyl nitrate (PAN) and its interaction with the
469 snowpack at Summit, Greenland, J. Geophys. Res., 107, ACH6, doi:10.1029/2001JD000547,
470 2002.
471 Frey, M. M., Brough, N., France, J. L., Anderson, P. S., Traulle, O., King, M. D., Jones, A. E.,
472 Wolff, E. W., and Savarino, J.: The diurnal variability of atmospheric nitrogen oxides (NO and
473 NO_2) above the Antarctic Plateau driven by atmospheric stability and snow emissions, Atmos.
474 Chem. Phys., 13, 3045-3042, doi:10.5194/acp-13-3045-2013, 2013.
475 Giglio, L., Randerson, J. T., and van der Werf, G. R.: Analysis of daily, monthly, and annual
476 burned area using the fourth-generation global fire emissions database (GFED4), J. Geophys.
477 Res. Biogeosci., 118, 1, 317-328, doi:10.1002/jgrg.20042, 2013.
478 Grannas, A. M., Jones, A. E., Dibb, J., Ammann, M., Anastasio, C., Beine, H. J., Bergin, M.,

Bottenheim, J., Boxe, C. S., Carver, G., Chen, G., Crawford, J. H., Domine, F., Frey, M. M., Guzman, M. I., Heard, D. E., Helmig, D., Hoffmann, M.R., Honrath, R. E., Huey, L. G., Hutterli, M., Jacobi, H. W., Klán, P., Lefer, B., McConnell, J., Plane, J., Sander, R., Savarino, J., Shepson, P. B., Simpson, W. R., Sodeau, J. R., von Glasow, R., Weller, R., Wolff, E. W., and Zhu, T.: An overview of snow photochemistry: evidence, mechanisms and impacts, Atmos. Chem. Phys., 7, 4329–4373, doi:10.5194/acp-7-4329-2007, 2007.

Guenther, A., Karl, T., Harley, P., Wiedinmyer, C., Palmer, P. I., and Geron C.: Estimate of global terrestrial isoprene emissions using MEGAN (Model of Emissions of Gases and Aerosols from Nature), Atmos. Chem. Phys., 6, 3181-3210, doi:10.5194/acp-6-3181-2006, 2006.

Helmig, D., Oltmans, S. J., Carlson, D., Lamarque, J. F., Jones, A., Labuschagne, C., Anlauf, K., Hayden, K.: A review of surface ozone in the polar regions, Atmospheric Environment, 41, 5138-5161, 2007a.

Helmig, D., Oltmans, S. J., Morse, T. O., and Dibb, J. E.: What is causing high ozone at Summit, Greenland?, Atmos. Environ., 41, 5031-5043, doi:10.1016/j.atmosenv.2006.05.084, 2007b.

Helmig, D., Ganzeveld, L., Butler, T., and Oltmans, S. J.: The role of ozone atmosphere-snow gas exchange on polar, boundary–layer tropospheric ozone- a review and sensitivity analysis, Atmos. Chem. Phys., 7, 15-30, doi:10.5194/acp-7-15-2007, 2007c.

Helmig, D., Johnson, B., Oltmans, S. J., Neff, W., Eisele, F., and Davis, D. D.: Elevated ozone in the boundary-layer at South Pole, Atmos. Environ., 42, 2788–2803, 2008.

Helmig, D., Petrenko, V., Martinerie, P., Witrant, E., Röckmann, T., Zuiderweg, A., Holzinger,

R., Hueber, J., Thompson, C., White, J. W. C., Sturges, W., Baker, A., Blunier, T., Etheridge, D., Rubino, M., and Tans, P.: Reconstruction of Northern Hemisphere 1950–2010 atmospheric non-methane hydrocarbons, Atmos. Chem. Phys., 14, 1463–1483, doi:10.5194/acp-14-1463-2014, 2014a.

Helmig, D., Stephens, C., Caramore, J., and Hueber, J.: Seasonal behavior of non-methane hydrocarbons in the firn air at Summit, Greenland, Atmos. Environ., 85, 234-246, doi:10.1016/j.atmosenv.2013.11.021, 2014b.

Hickman, J. E., Huang, Y., Wu, S., Diru, W., Groffman, P. M., Tully, K. L., and Palm, C. A.: Nonlinear response of nitric oxide fluxes to fertilizer inputs and the impacts of agricultural intensification on tropospheric ozone pollution in Kenya, Glob. Change Biol., 23, 3193-3204, doi:10.1111/gcb.13644, 2017.

Hollaway, M. J., Arnold, S. R., Challinor, A. J., and Emberson, L. D.: Intercontinental trans-boundary contributions to ozone-induced crop yield losses in the North Hemisphere, Biogeosciences, 9, 271-292, doi: 10.5194/bg-9-271-2012, 2012.

Honrath, R. E., Peterson, M. C., Guo, S., Dibb, J. E., Shepson, P. B., and Campbell, B.: Evidence of NO_x production within or upon ice particles in the Greenland snowpack, Geophys. Res. Lett., 26, 695-698, 1999.

Honrath, R. E., Guo, S., Peterson, M. C., Dziobak, M. P., Dibb, J. E., and Arsenault, M. A.: Photochemical production of gas phase NO_x from ice crystal NO_3^-, J. Geophys. Res., 105, 24183–24190, 2000a.

Honrath, R. E., Peterson, M. C., Dziobak, M. P., Dibb, J. E., Arsenault, M. A., and Green, S. A.:

Release of NO_x from Sunlight-irradiated Midlatitude Snow, Geophys. Res. Lett., 27, 2237–2240, 2000b.

Honrath, R. E., Lu, Y., Peterson, M. C., Dibb, J. E., Arsenault, M. A., Cullen, N. J., and Steffen, K.: Vertical fluxes of NO_x, HONO, and HNO_3 above the snowpack at Summit, Greenland, Atmos. Environ., 36, 2629-2640, doi:10.1016/S1352-2310(02)00132-2, 2002.

Huang, Y., Wu, S., Dubey, M. K., and French, N. H. F.: Impact of aging mechanism on model simulated carbonaceous aerosols, Atmos. Chem. Phys., 13, 6329–6343, doi:10.5194/acp-13-6329-2013, 2013.

Hudman, R. C., Moore, N. E., Mebust, A. K., Martin, R. V., Russell, A. R., Valin, L. C., and Cohen, R. C.: Steps towards a mechanistic model of global soil nitric oxide emissions: implementation and space based-constraints, Atmos. Chem. Phys., 12, 7779-7795, doi: 10.5194/acp-12-7779- 2012, 2012.

Hudman, R. C., Murray, L. T., Jacob, D. J., Turquety, S., Wu, S., Millet, D. B., Avery, M., Goldstein, A. H., and Holloway, J.: North American influence on tropospheric ozone and the effects of recent emission reductions: Constraints from ICARTT observations, J. Geophys. Res., 114, D07302, doi:10.1029/2008JD010126, 2009.

Jacob, D. J., Wofsy, S. C., Bakwin, P. S., Fan, S.-M., Harriss, R. C., Talbot, R. W., Bradshaw, J. D., Sandholm, S. T., Singh, H. B., Browell, E. V., Gregory, G. L., Sachse, G. W., Shipham, M. C., Blake, D. R., and Fitzjarrald, D. R.: Summertime photochemistry of the troposphere at high northern latitudes, J. Geophys. Res., 97, D15, 16421-16431, doi:10.1029/91JD01968, 1992.

Jang, J.-C., Jeffries, H., Byun, D., and Pleim, J.: Sensitivity of ozone to model grid resolution – I.

543 Application of high resolution regional acid deposition model, Atmos. Environ., 29, 3085-
544 3100, doi:10.1016/1352-2310(95)00118-I, 1995.
545 Johnson, M.S., Meskhidze, N., Solmon, F., Gasso, S., Chuang, P. Y., Gaiero, D. M., Yantosca,
546 R. M., Wu, S., Wang, X., Carouge, C.: Modeling Dust and Soluble Iron Deposition to the
547 South Atlantic Ocean, J. Geophys. Res., 115, D15202, doi:10.1029/2009JD013311, 2010.
548 Kramer, L. J., Helmig, D., Burkhart, J. F., Stohl, A., Oltmans, S., and Honrath, R. E.: Seasonal
549 variability of atmospheric nitrogen oxides and non-methane hydrocarbons at the GEOSummit
550 station, Greenland, Atmos. Chem. Phys., 15, 6827-6849, doi:10.5194/acp-15-6827-2015,
551 2015.
552 Kuhns, H., Knipping, E. M., and Vukovich, J. M.: Development of a United States-Mexico emis-
553 sions inventory for the Big Bend Regional Aerosol and Visibility Observational (BRAVO)
554 Study, JAPCA J. Air Waste M., 55, 677–692, 2005.
555 Kumar, A., Wu, S., Weise, M. F., Honrath, R., Owen, R. C., Helmig, D., Kramer, L., Val Martin,
556 M., and Li, Q.: Free-troposphere ozone and carbon monoxide over the North Atlantic for
557 2001–2011, Atmos. Chem. Phys., 13, 12537-12547, doi:10.5194/acp-13-12537-2013, 2013.
558 Legrand, M., Preunkert, S., Frey, M., Bartels-Rausch, Th., Kukui, A., King, M. D., Savarino, J.,
559 Kerbrat, M., and Jourdain, B.: Large mixing ratios of atmospheric nitrous acid (HONO) at
560 Concordia (East Antarctic Plateau) in summer: a strong source from surface snow?, Atmos.
561 Chem. Phys., 14, 9963-9976, doi:10.5194/acp-14-9963-2014, 2014.
562 Li, M., Zhang, Q., Kurokawa, J., Woo, J. H., He, K. B., Lu, Z., Ohara, T., Song, Y., Streets, D.
563 G., Carmichael, G. R., Cheng, Y. F., Hong, C. P., Huo, H., Jiang, X. J., Kang, S. C., Liu, F.,

564 Su, H., and Zheng, B.: MIX: a mosaic Asian anthropogenic emission inventory under the
565 international collaboration framework of the MICS-Asia and the HTAP, Atmos. Chem. Phys.,
566 17, 935-963, doi:10.5194/acpd-17-935-2017.
567 Liang, J., and Jacobson, M. Z.: Effects of subgrid segregation on ozone production efficiency in
568 a chemical model, Atmos. Environ., 34, 2975–2982, doi:10.1016/S1352-2310(99)00520-8,
569 2000.
570 Liang, Q., Rodriguez, J. M., Douglass, A. R., Crawford, J. H., Olson, J. R., Apel, E., Bian, H.,
571 Blake, D. R., Brune, W., Chin, M., Colarco, P. R., da Silva, A., Diskin, G. S., Duncan, B. N.,
572 Huey, L. G., Knapp, D. J., Montzka, D. D., Nielsen, J. E., Pawson, S., Riemer, D. D.,
573 Weinheimer, A. J., and Wisthaler, A.: Reactive nitrogen, ozone and ozone production in the
574 Arctic troposphere and the impact of stratosphere-troposphere exchange, Atmos. Chem. Phys.,
575 11, 13181-13199, doi:10.5194/acp-11-13181-2011, 2011.
576 Liu, H. Y., Jacob, D. J., Bey, I., and Yantosca, R. M.: Constraints from pb-210 and Be-7 on wet
577 deposition and transport in a global three-dimensional chemical tracer model driven by
578 assimilated meteorological fields, J. Geophys. Res.-Atmos., 106, 12109-12128, doi:
579 10.1029/2000JD900839, 2001.
580 Martin, R. V., Jacob, D. J., Logan, J. A., Bey, I., Yantosca, R. M., Staudt, A. C., Li, Q., Fiore, A.
581 M., Duncan, B. N., and Liu, H.: Interpretation of TOMS observations of tropical tropospheric
582 ozone with a global model and in situ observations, J. Geophys. Res., 107(D18), ACH 4-1-
583 ACH 4-27, doi: 10.1029/2001JD001480, 2002.
584 McClure-Begley, A., Petropavlovskikh, I., Oltmans, S.: NOAA Global Monitoring Surface

585 Ozone Network. 1973-2014. National Oceanic and Atmospheric Administration, Earth
586 Systems Research Laboratory Global Monitoring Division. Boulder, CO. DATE ACCESSED:
587 4/23/2017, http://dx.doi.org/10.7289/V57P8WBF, 2014.
588 McLinden, C. A., Olsen, S. C., Hannegan, B., Wild, O., Prather, M. J., and Sundet, J.:
589 Stratospheric ozone in 3-D models: A simple chemistry and the cross-tropopause flux, J.
590 Geophys. Res., 105, D11, 14653-14665, doi:10.1029/2000JD900124, 2000.
591 Monks, S. A., Arnold, S. R., Emmons, L. K., Law, K. S., Turquety, S., Duncan, B. N.,
592 Flemming, J., Huijnen, V., Tilmes, S., Langner, J., Mao, J., Long, Y., Thomas, J. L., Steenrod,
593 S. D., Raut, J. C., Wilson, C., Chipperfield, M. P., Diskin, G. S., Weinheimer, A., Schlager,
594 H., and Ancellet, G.: Multi-model study of chemical and physical controls on transport of
595 anthropogenic and biomass burning pollution to the Arctic, Atmos. Chem. Phys., 15, 3575-
596 3603, doi:10.5194/acp-15-3575-2015, 2015.
597 Murray, K. A., Kramer, L. J., Doskey, P. V., Ganzeveld, L., Seok, B., Van Dam, B., and Helmig,
598 D.: Dynamics of ozone and nitrogen oxides at Summit, Greenland. II. Simulating snowpack
599 chemistry during a spring high ozone event with a 1-D process-scale model, Atmos. Environ.,
600 117, 110–123, doi:10.1016/j.atmosenv.2015.07.004, 2015.
601 Murray, L. T., Jacob, D. J., Logan, J. A., Hudman, R. C., and Koshak, W. J.: Optimized regional
602 and interannual variability of lightning in a global chemical transport constrained by LIS/OTD
603 satellite data, J. Geophys. Res., 117, D20307, doi:10.1029/2012JD017934, 2012.
604 Novelli, P. C. and Masarie, K. A.: Atmospheric Carbon Monoxide Dry Air Mole Fraction from
605 the NOAA ESRL Carbon Cycle Cooperative Global Air Sampling Network, 1988-2014,

606 Version: 2015-08-04, NOAA, available at
607 ftp://aftp.cmdl.noaa.gov/data/trace_gases/co/flask/surface/, 2015.
608 Park, R. J., Jacob, D. J., Field, B. D., Yantosca, R. M., and Chin, M.: Natural and transboundary
609 pollution influences on sulfate-nitrate-ammonium aerosols in the United States: Implications
610 for policy, J. Geophys. Res.-Atmos., 109, D15204, doi:10.1029/2003JD004473, 2004.
611 Petropavlovskikh, I. and Oltmans, S. J.: Tropospheric Ozone Measurements, 1973-2011,
612 Version: 2012-07-10, NOAA, available at: ftp://aftp.cmdl.noaa.gov/data/ozwv/SurfaceOzone/,
613 2012.
614 Price, C. and Rind, D.: A simple lightning parameterization for calculating global lightning
615 distributions, J. Geophys. Res., 97, 9919-9933, doi:10.1029/92JD00719,1992.
616 Ridley, B. A., and Grahek, F.: A small, low flow, high sensitivity reaction vessel for NO
617 chemiluminescence detectors, Am. Meteorol. Soc., 7, 307-311, 1990.
618 Sauvage, B., Martin, R. V., van Donkelaar, A., Liu, X., Chance, K., Jaeglé, L., Palmer, P. I., Wu,
619 S., and Fu, T.-M.: Remote sensed and in situ constraints on processes affecting tropical tropo-
620 spheric ozone, Atmos. Chem. Phys., 7, 815–838, doi:10.5194/acp-7-815-2007, 2007.
621 Sherwen, T., Schmidt, J. A., Evans, M. J., Carpenter, L. J., Groß- mann, K., Eastham, S. D.,
622 Jacob, D. J., Dix, B., Koenig, T. K., Sinreich, R., Ortega, I., Volkamer, R., Saiz-Lopez, A.,
623 Prados-Roman, C., Mahajan, A. S., and Ordóñez, C.: Global impacts of tropospheric halogens
624 (Cl, Br, I) on oxidants and composi- tion in GEOS-Chem, Atmos. Chem. Phys., 16, 12239–
625 12271, doi:10.5194/acp-16-12239-2016, 2016.
626 Shindell, D. T., Chin, M., Dentener, F., Doherty, R. M., Faluvegi, G., Fiore, A. M., Hess, P.,

627 Koch, D. M., MacKenzie, I. A., Sanderson, M. G., Schultz, M., Stevenson, D. S., Teich, H.,
628 Textor, C., Wild, O., Bergmann, D. J., Bey, I., Bian, H., Cuvelier, C., Duncan, B. N., Folberth,
629 G., Horowitz, L. W., Jonson, J., Kaminski, J. W., Marmer, E., Park, R., Pringle, K. J.,
630 Schroeder, S., Szopa, S., Takemura, T., Zeng, G., Keating, T. J., and Zuber, A.: A multi-model
631 assessment of pollution transport to the Arctic, Atmos. Chem. Phys., 8, 5353-5372,
632 doi:10.5194/acp-8-5353-2008, 2008.
633 Simon, H., Beck, L., Bhave, P. V., Divita, F., Hsu, Y., Luecken, D., Mobley, J. D., Pouliot, G.
634 A., Reff, A., Sarwar, G., and Strum, M.: The development and uses of EPA's SPECIATE
635 database, Atmospheric Pollution Research, 196-206, 10.5094/apr.2010.026, 2010.
636 Thomas, J. L., Stutz, J., Lefer, B., Huey, L. G., Toyota, K., Dibb, J. E., and von Glasow, R.:
637 Modeling chemistry in and above snow at Summit, Greenland – Part 1: Model description and
638 results, Atmos. Chem. Phys., 11, 4899–4914, doi:10.5194/acp-11-4899- 2011, 2011.
639 Thomas, J. L., Dibb, J. E., Huey, L. G., Liao, J., Tanner, D., Lefer, B., von Glasow, R., and
640 Stutz, J.: Modeling chemistry in and above snow at Summit, Greenland – Part 2: Impact of
641 snowpack chemistry on the oxidation capacity of the boundary layer, Atmos. Chem. Phys., 12,
642 6537–6554, doi:10.5194/acp-12-6537-2012, 2012.
643 Tzompa-Sosa, Z. A., Mahieu, E., Franco, B., Keller, C. A., Turner, A. J., Helmig, D., Fried, A.,
644 Richter, D., Weibring, P., Walega, J., Yacovitch, T. I., Herndon, S. C., Blake, D. R., Hase, F.,
645 Hannigan, J. W., Conway, S., Strong, K., Schneider, M., and Fischer, E. V.: Revisiting global
646 fossil fuel and biofuel emissions of ethane, J. Geophys. Res. Atmos., 122,
647 doi:10.1002/2016JD025767, 2017.

Unger, N., Shindell, D. T., Koch, D. M., and Streets, D. G.: Cross influences of ozone and sulfate precursor emissions changes on air quality and climate, Proc. Natl. Acad. Sci., 103, 4377-4380, doi:10.1073/pnas.0508769103, 2006.

van het Bolscher, M., Pereira, J., Spesso, A., Dalsoren, S., van Noije, T., and Szopa, S.: REanalysis of the TROpospheric chemical composition over the past 40 years: A long-term global modeling study of tropospheric chemistry, Max Plank Inst. For Meteorology, Hamburg, Germany, 77, 2008.

Van Dam, B., Helmig, D., Toro, C., Doskey, P., Kramer, L., Murray, K., Ganzeveld, L., and Seok, B.: Dynamics of ozone and nitrogen oxides at Summit, Greenland: I. Multi-year observations in the snowpack, Atmos. Environ., 123, 268-284, doi:10.1016/j.atmosenv.2015.09.060, 2015.

Walker, T. W., Jones, D. B. A., Parrington, M., Henze, D. K., Murray, L. T., Bottenheim, J. W., Anlauf, K., Worden, J. R., Bowman, K. W., Shim, C., Singh, K., Kopacz, M., Tarasick, D. W., Davies, J., von der Gathen, P., Thompson, A. M., and Carouge, C. C.: Impacts of midlatitude precursor emissions and local photochemistry on ozone abundances in the Arctic, J. Geophys. Res., 117, D01305, doi:10.1029/2011JD016370, 2012.

Wang, Y. H., Jacob, D. J., and Logan, J. A.: Global simulation of tropospheric O_3-NOx-hydro-carbon chemistry 1. Model formulation, J. Geophys. Res.-Atmos., 103, 10713-10725, doi: 10.1029/98JD00158, 1998.

Wang, Y. X., McElroy, M. B., Jacob, D. J., and Yantosca, R. M.: A nested grid formulation for chemical transport over Asia: Applications to CO, J. Geophys. Res., 109, D22307,

669 doi:10.1029/2004JD005237, 2004.
670 Wesely, M. L.: Parameterization of surface resistances to gaseous dry deposition in regional-
671 scale numerical-models, Atmos. Environ., 23, 1293-1304, doi:10.1016/0004-6981(89)90153-
672 4, 1989.
673 Wespes, C., Emmons, L., Edwards, D. P., Hannigan, J., Hurtmans, D., Saunois, M., Coheur, P.-
674 F., Clerbaux, C., Coffey, M. T., Batchelor, R. L., Lindenmaier, R., Strong, K., Weinheimer, A.
675 J., Nowak, J. B., Ryerson, T. B., Crounse, J. D., and Wennberg, P. O.: Analysis of ozone and
676 nitric acid in spring and summer Arctic pollution using aircraft, ground-based, satellite
677 observations and MOZART-4 model: source attribution and partitioning, Atmos. Chem. Phys.,
678 12, 237–259, doi:10.5194/acp- 12-237-2012, 2012.
679 Wu, S., Mickley, L. J., Jacob, D. J., Logan, J. A., Yantosca, R. M., and Rind, D.: Why are there
680 large differences between models in global budgets of tropospheric ozone?, J. Geophys. Res.,
681 112(D5), D05302, doi:10.1029/02006JD007801, 2007.
682 Xiao, Y., Logan, J. A., Jacob, D. J., Hudman, R. C., Yantosca, R., and Blake, D. R.: The global
683 budget of ethane and regional constrainsts on U.S. sources, J. Geophys. Res., 113, D21306,
684 doi:10.1029/2007JD009415, 2008.
685 Yang, J., Honrath, R. E., Peterson, M. C., Dibb, J. E., Sumner, A. L., Shepson, P. B., Frey, M.,
686 Jacobi, H.-W., Swanson, A., and Blake, N.: Impacts of snowpack emissions on deduced levels
687 of OH and peroxy radicals at Summit, Greenland, Atmos. Environ., 36, 2523-2534,
688 doi:10.1016/S1352-2310(02)00128-0, 2002.
689 Yevich, R., and Logan, J. A.: An assesment of biofuel use and burning of agricultural waste in

the developing world, Global Biogeochem. Cy., 17, 1095, doi:10.1029/2002GB001952, 2003.

Yu, K., Jacob, D. J., Fisher, J. A., Kim, P. S., Marais, E. A., Miller, C. C., Travis, K. R., Zhu, L., Yantosca, R. M., Sulprizio, M. P., Cohen, R. C., Dibb, J. E., Fried, A., Mikoviny, T., Ryerson, T. B., Wennberg, P. O., and Wisthaler, A.: Sensitivity to grid resolution in the ability of a chemical transport model to simu- late observed oxidant chemistry under high-isoprene conditions, Atmos. Chem. Phys., 16, 4369–4378, doi:10.5194/acp-16-4369- 2016, 2016.

Zatko, M. C., Geng, L., Alexander, B., Sofen, E. D., and Klein, K.: The impact of snow nitrate photolysis on boundary layer chemistry and the recycling and redistribution of reactive nitrogen across Antarctica and Greenland in a global chemical transport model, Atmos. Chem. Phys., 16, 2819-2842, doi:10.5194/acpd-16-2819-2016, 2016.

Zhang, H., Wu, S., Huang, Y., and Wang, Y.: Effects of stratospheric ozone recovery on photochemistry and ozone air quality in the troposphere, Atmos. Chem. Phys., 14, 4079-4086, doi:10.5194/acp-14-4079-2014, 2014.

Zhou, X., Beine, H. J., Honrath, R. E., Fuentes, J., Simpson, W., Shepson, P. B., and Bottenheim, J. W.: snowpack photochemical production of HONO: a major source of OH in the Arctic boundary layer in springtime, Geophys. Res. Lett., 28, 21, 4087-4090, 2001.

711 **Table 1.** Surface NO_2 measurements over Europe during 2009/12/01-2010/01/31.

Site ID	Site name	Lat. (°N)	Lon. (°E)	Altitude a.s.l (m)	Technique	Resolution
BE0001R	Offagne	49.88	5.20	430	chemiluminescence	hourly
BE0032R	Eupen	50.63	6	295	chemiluminescence	hourly
DE0001R	Westerland	54.93	8.31	12	NaJ_solution	daily
DK0008R	Anholt	56.72	11.52	40	UV_fluorescence	hourly
FI0096G	Pallas	67.97	24.12	340	chemiluminescence	hourly
GB0014R	High Muffles	54.33	-0.8	267	chemiluminescence	daily
NL0009R	Kollumerwaard	53.33	6.28	1	chemiluminescence	hourly
NO0001R	Birkenes	58.38	8.25	190	glass sinter	daily
NO0039R	Kårvatn	62.78	8.88	210	glass sinter	daily
NO0056R	Hurdal	60.37	11.08	300	glass sinter	daily
SE0005R	Bredkälen	63.85	15.3	404	abs_tube	daily

712

713

714

715

716

717

718

719

720

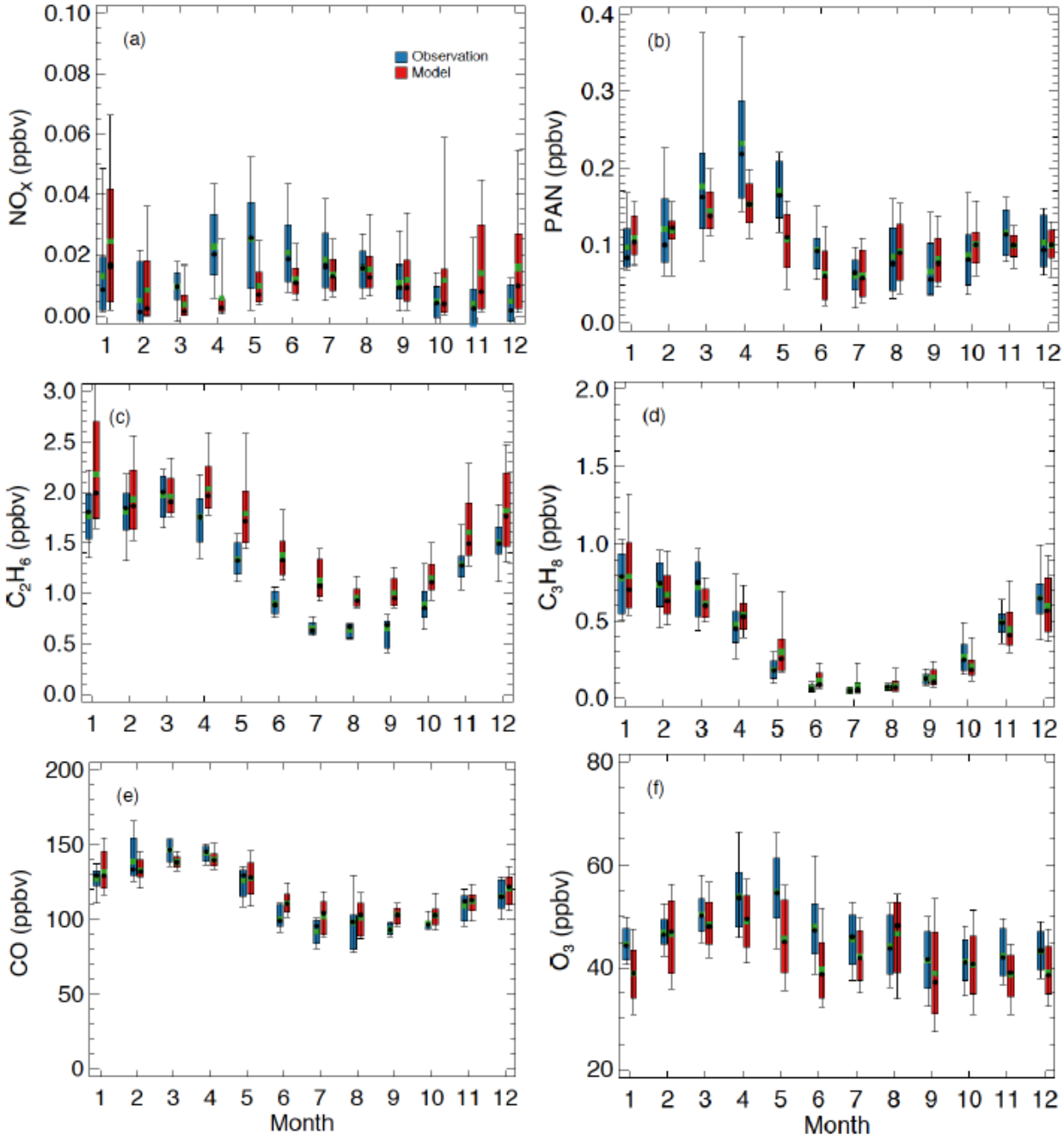

721

722 **Fig. 1.** Box plot comparison for seasonal variations of (a) NO_x, (b) PAN, (c) C_2H_6, (d) C_3H_8, (e)
723 CO, and (f) O_3 between GEOS-Chem model simulations (red) and measurements (blue) at
724 Summit for the period of 2008/07-2010/06. Data shown are monthly averages during this period.
725 The thick (thin) bars represent the 67% (95%) confidence intervals. Black and green dots
726 represent median and mean values, respectively. The statistics are based on daily averages.

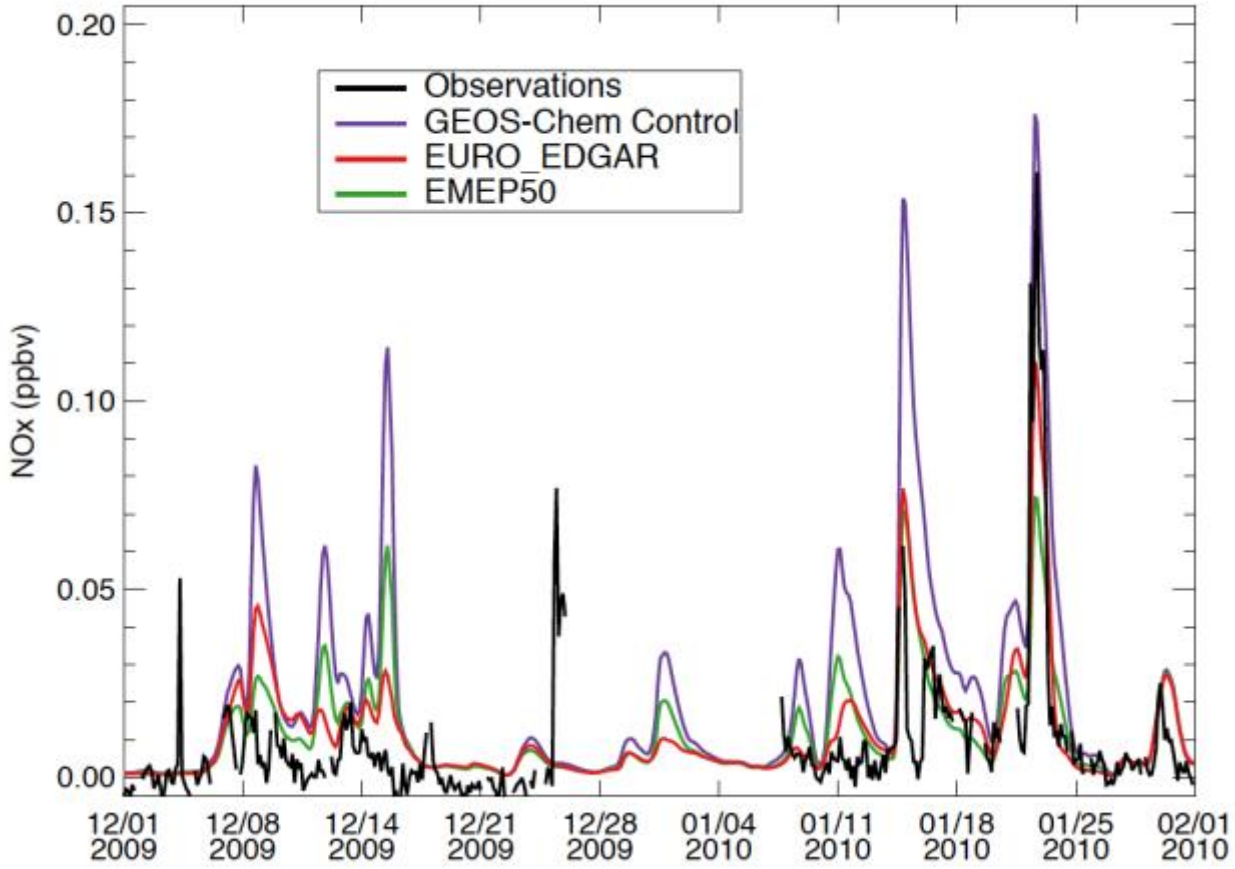

Figure 2. Timeseries of surface NO_x mixing ratios over Summit from observations, GEOS-Chem model control simulations, EURO_EDGAR, and EMEP50 during 2009/12/01-2010/01/31. EURO_EDGAR represents simulations with anthropogenic NO_x emissions over Europe following EDGAR v4.2, while EMEP50 denotes simulations with anthropogenic NO_x emissions from the EMEP emission inventory over Europe reduced by 50%, with other model configurations identical to the control simulations. Readers are referred to the text for details.

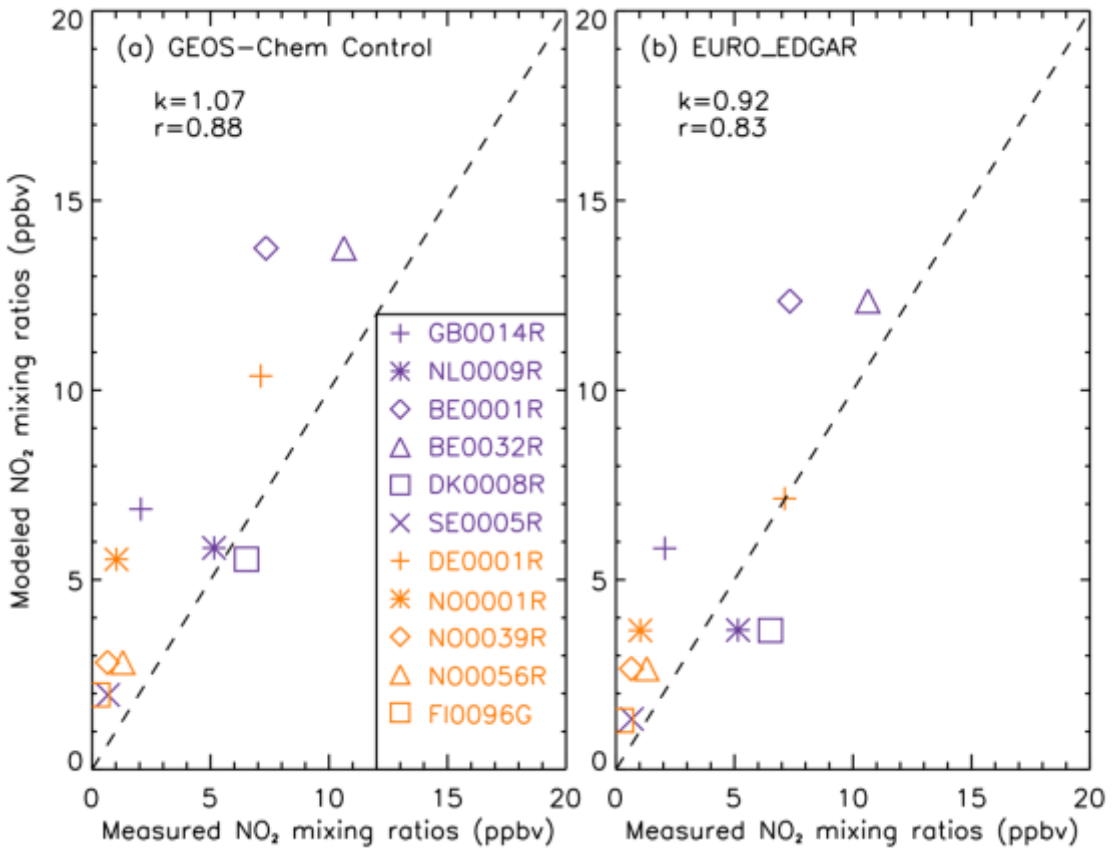

739

740 **Figure 3.** Scatter plots of model simulations from (a) GEOS-Chem control simulations and (b)
741 EURO_EDGAR during 2009/12/01-2010/01/31 and measured monthly mean NO_2 mixing ratios
742 at 11 observational sites over Europe; also shown is the corresponding model-to-observation
743 slopes (k) and correlation coefficients (r) for each panel. The dashed line is the 1:1 ratio.
744 Explanations of site abbreviations are listed in Table 1. EURO_EDGAR represents simulations
745 with anthropogenic NO_x emissions over Europe following EDGAR v4.2, with other model
746 configurations identical to the control simulations.

747

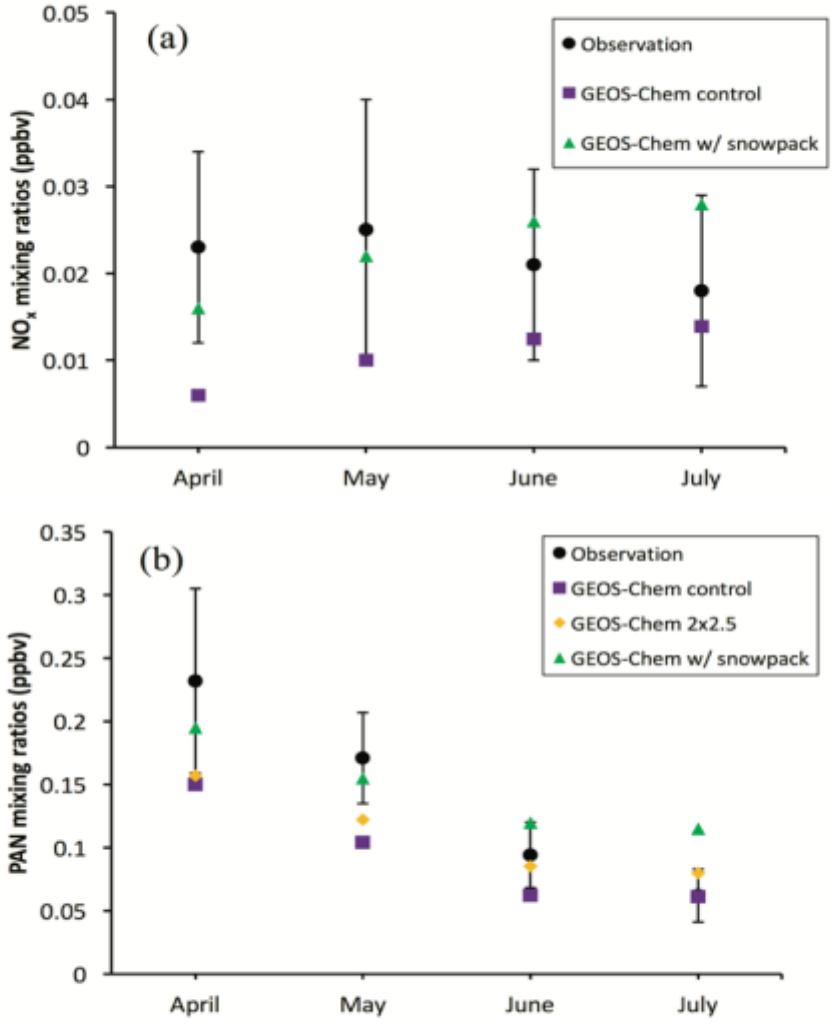

748

749 **Figure 4.** Monthly mean surface (a) NO_x and (b) PAN mixing ratios from observations (black
750 circles), simulations with (green triangles) /without (purple squares) snowpack emissions, and
751 GEOS-Chem simulations with horizontal grid resolution 2° x 2.5° (orange diamonds) for April-
752 July during 07/2008-06/2010. Vertical bars denote standard deviations over the course of
753 observations for each month.

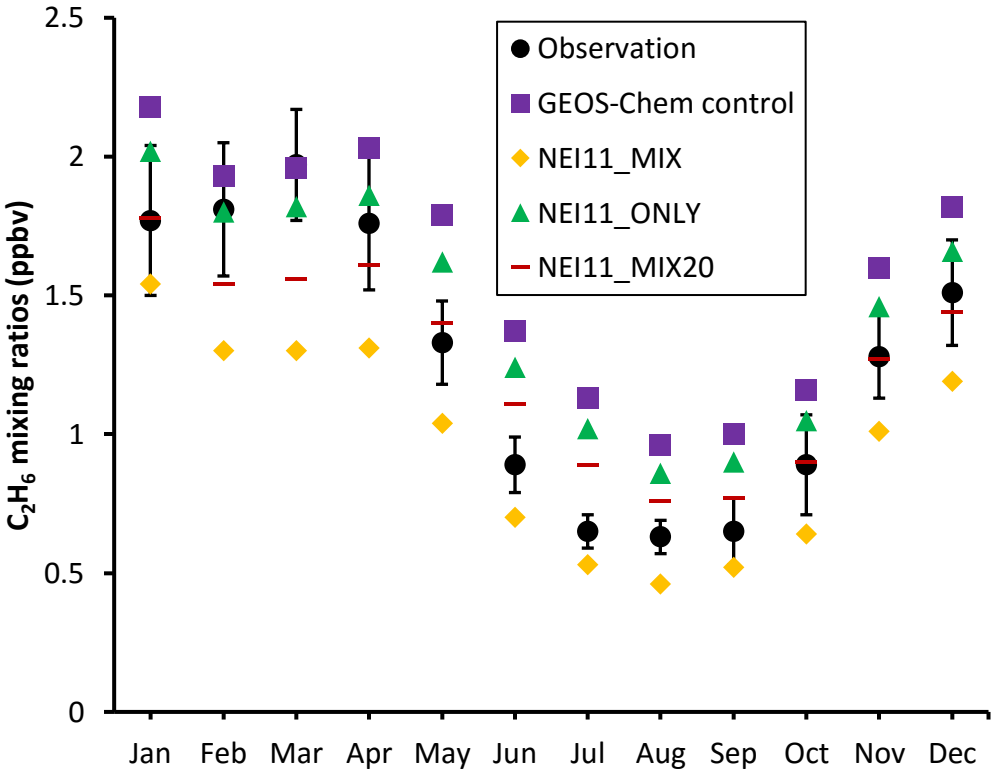

754

755 **Figure 5**. Monthly mean surface C_2H_6 mixing ratios at Summit from observations (black
756 circles), GEOS-Chem model control simulations (purple squares), NEI11_MIX (orange
757 diamond), and NEI11_ONLY (green triangles) simulations during 2008-2010; vertical bars
758 denote the standard deviation over the course of observations for each month. NEI11_MIX
759 represents model perturbations with global C_2H_6 emission inventories overwritten by NEI11 over
760 US and by MIX over Asia, with other model configurations identical to the control simulations.
761 NEI11_ONLY denotes the simulation that is the same with the control simulation except that the
762 C_2H_6 emission inventory over US is overwritten by NEI11. NEI11_MIX20 is the simulation that
763 is identical to NEI11_MIX except the 20% increased MIX C_2H_6 emission inventory over Asia.
764 Readers are referred to the text for details.

765

766

767

768

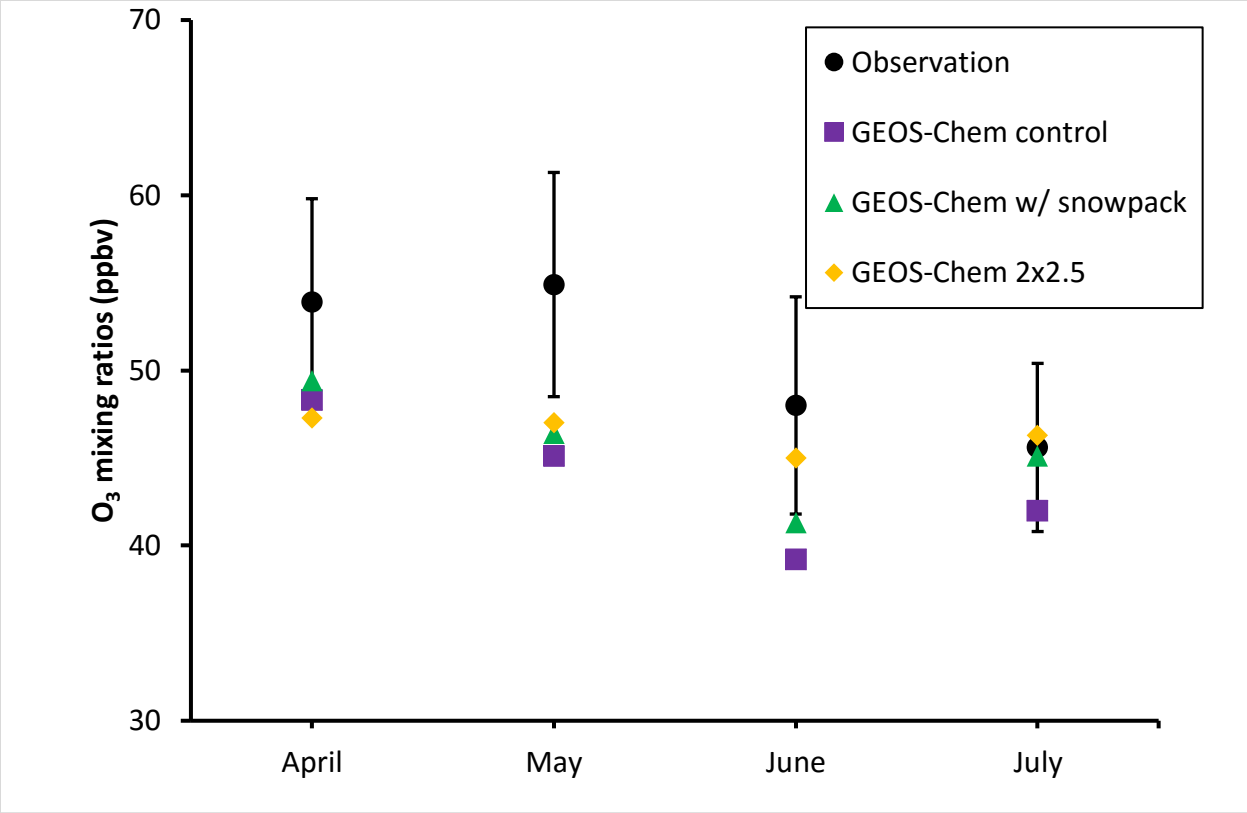

Figure 6. Monthly mean surface O_3 mixing ratios from observations (black circles), GEOS-Chem control runs (purple squares), with snowpack chemistry (green triangles), and horizonal grid resolution 2° x 2.5° (orange diamonds) for April-July. Vertical bars denote the variability over the course of observations for each month.

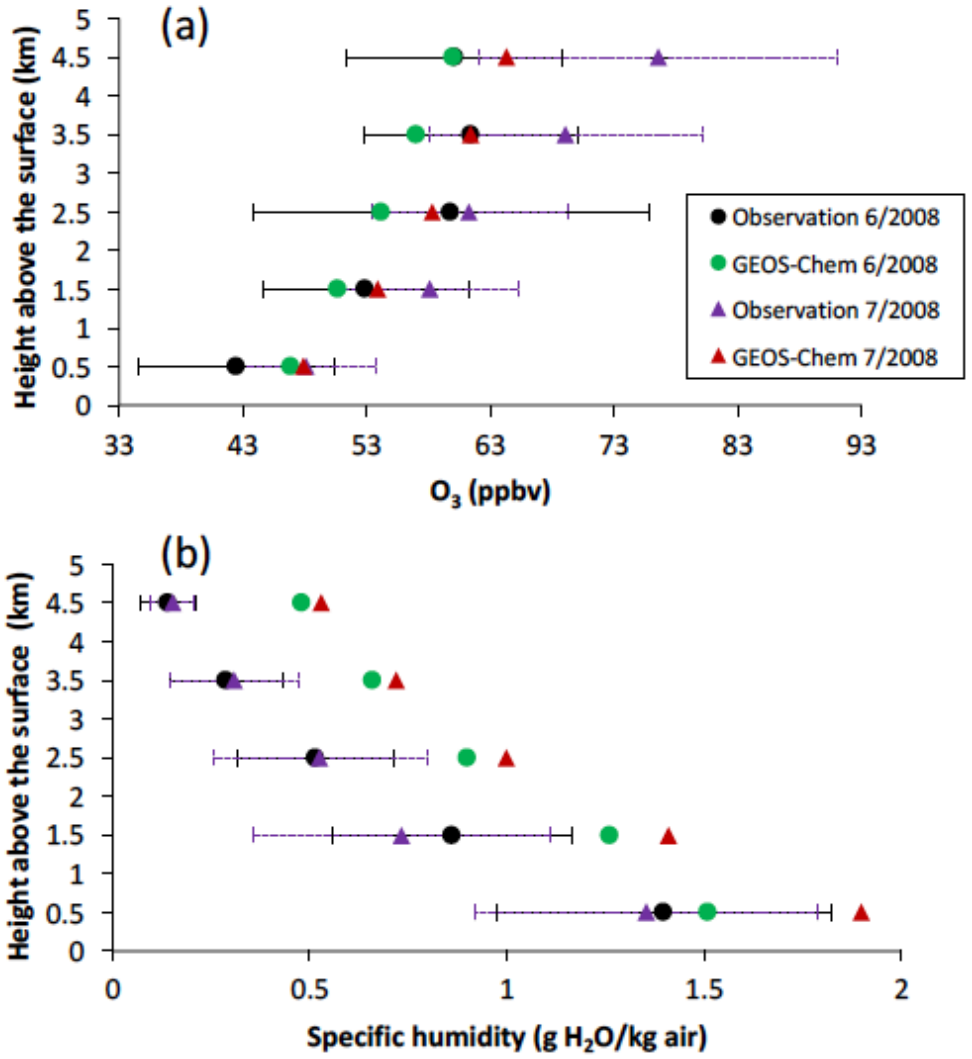

782

783 **Figure 7.** Comparisons of vertical profiles of (a) O_3 and (b) specific humidity between GEOS-
784 Chem simulations and ozonesondes in June and July 2008 respectively, averaged over 1-km
785 altitude bins. Black and green solid circles represent observations and simulations in June 2008
786 while purple and red triangles denote observations and simulations for July 2008 respectively.
787 Solid and dashed horizontal error bars represent observational standard deviations for June and
788 July respectively.

789